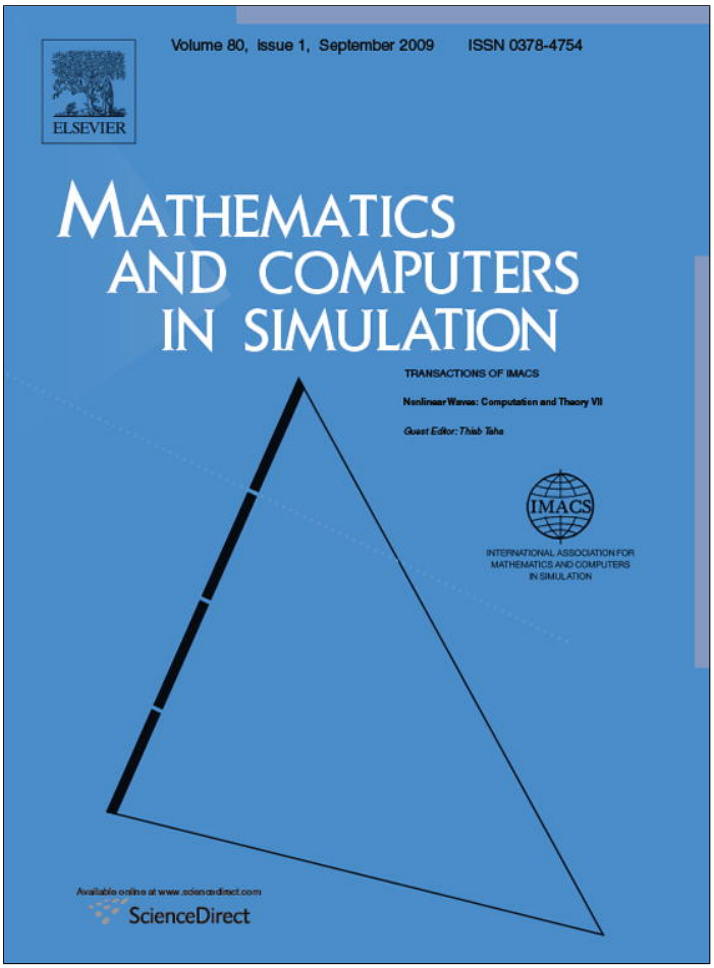

Available online at www.sciencedirect.com
ScienceDirect
Mathematics and Computers in Simulation 80 (2009) 29–36
MATHEMATICS AND COMPUTERS IN SIMULATION
www.elsevier.com/locate/matcom

Nonlinear surface waves interacting with a linear shear current

Wooyoung Choi *

Department of Mathematical Science, Center for Applied Mathematics and Statistics, New Jersey Institute of Technology, Newark, NJ 07102-1982, United States

Available online 18 June 2009

Abstract

To describe the evolution of fully nonlinear surface gravity waves in a linear shear current, a closed system of exact evolution equations for the free surface elevation and the free surface velocity potential is derived using a conformal mapping technique. Traveling wave solutions of the system are obtained numerically and it is found that the maximum wave amplitude for a positive shear current is much smaller than that in the absence of any shear while the opposite is true for a negative shear current. The new evolution equations are also solved numerically using a pseudo-spectral method to study the Benjamin–Feir instability of a modulated wave train in both positive and negative shear currents. With a fixed wave slope, compared with the irrotational case, the envelope of the modulated wave train grows faster in a positive shear current and slower in a negative shear current.

Keywords: Nonlinear surface waves; Linear shear current; Benjamin-Feir instability

1. Introduction

We consider fully nonlinear water waves propagating in a linear shear current and study the effect of background shear on the evolution of a modulated wave train using a new set of exact evolution equations.

Understanding the interaction of surface gravity-capillary waves with non-uniform currents is of great importance for oceanic and remote sensing applications [13], but the evolution of surface waves in a vertically varying current has attracted much less attention than that in a horizontally varying current. Vertically sheared flows are in general strongly rotational and, therefore, a theoretical description of unsteady surface waves in such flows is non-trivial, in particular, when nonlinear effects become important. To better understand how a vertically varying current affects the evolution of highly nonlinear waves, we consider here a relatively simple current profile of constant vorticity for which all two-dimensional perturbations are irrotational and, therefore, mathematical approaches to study fully nonlinear irrotational water waves can be readily generalized.

For periodic traveling waves, the fully nonlinear steady wave solutions of the Euler equations in a uniform shear current were computed numerically by Dalrymple (1974), Simmen and Saffman (1985) [6,15] and Vanden-Broeck (1996) [19], and their linear stability characteristics were studied by Pullin and Grimshaw (1986) [14] and Okamura and Oikawa (1989) [11]. Solitary waves solutions were also obtained numerically by Teles da Silva and Peregrine (1988) [17] and Vanden-Broeck (1994) [18]. Asymptotic theories for steady waves were presented, for example, by Tsao (1959) for periodic waves, and by Benjamin (1962), Miroshinikov (2002) [3,10] and Choi (2003) [4] for solitary waves.

* Corresponding author.
E-mail address: wychoi@njit.edu.

0378-4754/$36.00
doi:10.1016/j.matcom.2009.06.021

The evolution of fully nonlinear surface waves in a uniform shear current on the other hand has been studied much less extensively while Banner and Song (2002) [1] and Banner and Tian (1998) [2] studied the onset of wave breaking under the influence of a uniform shear flow using the numerical model of Dold and Peregrine (1986) [7] based on a boundary element method. In this paper, we present an alternative formulation that leads to a closed system of two coupled nonlinear evolution equations for which both steady and unsteady numerical solutions can be found easily using a pseudo-spectral method.

In the absence of shear, Ovsjannikov (1974) [12] first showed that it is possible to reduce the fully nonlinear Euler equations to a closed system of exact evolution equations for the free surface elevation and the free surface velocity potential by using a conformal mapping technique. This system was also obtained later by Dyachenko, Zakharov and Kuznetsov (1996) [8]. For the case of constant vorticity, since the wave motions are irrotational, the approach to derive the system of nonlinear evolution equations for irrotational waves can be readily applied, with a slight modification, to the case of our interest.

With a system of exact evolution equations derived in Section 2, we obtain traveling wave solutions and study the Benjamin–Feir instability in Section 3 using pseudo-spectral methods similar to those for steady and unsteady irrotational water waves adopted by Choi and Camassa (1999) [5] and Li, Hyman and Choi (2004) [9], respectively.

2. Mathematical formulation

The basic flow of interest is a uniform shear flow given by

$$U(y) = U_0 + \Omega y \qquad \text{for } -h \le y \le 0, \tag{2.1}$$

where U_0 is a constant velocity at the mean free surface and the case of positive Ω is referred to as a positive shear. Since the vorticity $(-\Omega)$ of this basic flow is constant, it can be shown that the velocity field induced by a two-dimensional perturbation must be irrotational from conservation of vorticity. Then, we can introduce the velocity potential $\hat{\phi}(x, y, t)$ for the perturbation, which satisfies the Laplace equation and the boundary conditions at the free surface and at the flat bottom:

$$\hat{\phi}_{xx} + \hat{\phi}_{yy} = 0 \qquad \text{for } -h \le y \le \zeta, \tag{2.2}$$

$$\zeta_t + (U_0 + \Omega\zeta + \hat{\phi}_x)\zeta_x = \hat{\phi}_y \quad \text{at } y = \zeta(x, t), \tag{2.3}$$

$$\hat{\phi}_t + g\zeta + \frac{1}{2}\left(\hat{\phi}_x^2 + \hat{\phi}_y^2\right) + (U_0 + \Omega\zeta)\,\hat{\phi}_x - \Omega\hat{\psi} = \frac{\sigma}{\rho}\frac{\zeta_{xx}}{(1+\zeta_x{}^2)^{3/2}} \quad \text{at } y = \zeta(x, t), \tag{2.4}$$

$$\hat{\phi}_y = 0 \quad \text{at } y = -h, \tag{2.5}$$

where $\zeta(x, t)$ is the free surface elevation, $\hat{\psi}$ is the perturbation streamfunction, g is the gravitational acceleration, σ is the surface tension, h is the water depth, and the subscript denotes differentiation. The dynamic boundary condition given by (2.4) is obtained from the Bernoulli equation for a rotational flow with constant vorticity.

To solve the problem, we first introduce a transformation that maps conformally the physical domain shown in Fig. 1 onto a horizontal strip of uniform thickness h:

$$x = x(\xi, \eta, t), \qquad y = y(\xi, \eta, t). \tag{2.6}$$

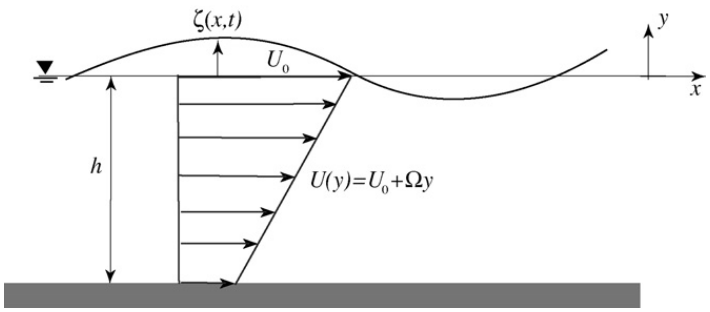

Fig. 1. Surface waves in a linear shear current.

Under this transformation, the free surface is mapped onto the flat surface at $\eta = 0$, and the kinematic and dynamic free surface boundary conditions, (2.3)–(2.4), can be rewritten as

$$x_\xi\, y_t - y_\xi\, x_t = -\psi_\xi - (U_0 + \Omega y)\, y_\xi \qquad \text{at } \eta = 0, \tag{2.7}$$

$$\begin{aligned} &\phi_t + gy + \frac{1}{J}\left[-(x_\xi x_t + y_\xi y_t)\phi_\xi + (x_\xi y_t - y_\xi x_t)\psi_\xi + \frac{1}{2}{\phi_\xi}^2 + \frac{1}{2}{\psi_\xi}^2\right] \\ &+\frac{1}{J}(U_0 + \Omega y)(x_\xi \phi_\xi + y_\xi \psi_\xi) - \Omega\psi = \frac{\sigma}{\rho}\frac{x_\xi y_{\xi\xi} - y_\xi x_{\xi\xi}}{({x_\xi}^2 + {y_\xi}^2)^{3/2}} \quad \text{at } \eta = 0, \end{aligned} \tag{2.8}$$

where $y(\xi, 0, t) \equiv \zeta(x(\xi, 0, t), t)$ is the free surface elevation, the Jacobian J is given by

$$J = {x_\xi}^2 + {y_\xi}^2, \tag{2.9}$$

and ϕ and ψ are the velocity potential and the streamfunction, respectively, evaluated at the free surface:

$$\phi(\xi, \eta, t) \equiv \hat{\phi}(x(\xi, \eta, t), y(\xi, \eta, t), t), \qquad \psi(\xi, \eta, t) \equiv \hat{\psi}(x(\xi, \eta, t), y(\xi, \eta, t), t). \tag{2.10}$$

To obtain (2.7)–(2.8) from (2.3)–(2.4), we have used the Cauchy–Riemann relationships: $x_\xi = y_\eta$ and $x_\eta = -y_\xi$.

Since the left-hand side of Eq. (2.7) divided by J is the imaginary part of (z_t/z_ξ), which is harmonic, the real part of (z_t/z_ξ) can be found from the relationship between the real and imaginary parts of a harmonic function in a strip of thickness h given by

$$\mathrm{Re}\,(z_t/z_\xi) = -\mathcal{T}[\mathrm{Im}\,(z_t/z_\xi)], \tag{2.11}$$

where operator $\mathcal{T}$ is defined by

$$\mathcal{T}[f] = \frac{1}{2h}\int_{-\infty}^{\infty} f(\xi', 0, t)\, \coth\left[\frac{\pi}{2h}(\xi' - \xi)\right] \mathrm{d}\xi', \tag{2.12}$$

which, for infinitely deep water ($h \to \infty$), becomes the Hilbert transform $\mathcal{H}$ given by

$$\mathcal{H}[f] = \frac{1}{\pi}\int_{-\infty}^{\infty} \frac{f(\xi', 0, t)}{\xi' - \xi}\mathrm{d}\xi'. \tag{2.13}$$

From (2.7) and (2.11), the real part of (z_t/z_ξ) can be found as

$$x_\xi\, x_t + y_\xi\, y_t = J\,\mathcal{T}\left[\frac{\Psi_\xi}{J}\right] \qquad \text{at } \eta = 0, \tag{2.14}$$

where Ψ_ξ is defined as

$$\Psi_\xi \equiv \psi_\xi + U_0 y_\xi + \Omega y y_\xi. \tag{2.15}$$

Then, by solving (2.7) and (2.14) for x_t and y_t, the evolution equations for $x(\xi, 0, t)$ and $y(\xi, 0, t)$ can be obtained as

$$x_t = x_\xi\,\mathcal{T}\left[\frac{\Psi_\xi}{J}\right] + y_\xi\,\frac{\Psi_\xi}{J}, \tag{2.16}$$

$$y_t = y_\xi\,\mathcal{T}\left[\frac{\Psi_\xi}{J}\right] - x_\xi\,\frac{\Psi_\xi}{J}. \tag{2.17}$$

On the other hand, using (2.16)–(2.17), the dynamic free surface boundary condition (2.8) yields the evolution equation for $\phi(\xi, 0, t)$:

$$\phi_t = -gy - \frac{1}{2J}({\phi_\xi}^2 - {\psi_\xi}^2) + \phi_\xi\mathcal{T}\left[\frac{\Psi_\xi}{J}\right] - \frac{1}{J}(U_0 + \Omega y)x_\xi\phi_\xi + \Omega\psi + \frac{\sigma}{\rho}\frac{x_\xi y_{\xi\xi} - y_\xi x_{\xi\xi}}{({x_\xi}^2 + {y_\xi}^2)^{3/2}}. \tag{2.18}$$

Notice that the steady translation of the reference frame with constant speed U_0 in the physical plane produces nonlinear terms in the evolution equations in the transformed plane. Since $z = x + iy$ and $w = \phi + i\psi$ are also harmonic functions

in the transformed plane whose real and imaginary parts at the free surface (or at $\eta = 0$ in the transformed plane) are related, from (2.11), as

$$x_\xi - 1 = -\mathcal{T}[y_\xi]\,, \qquad \phi_\xi = -\mathcal{T}[\psi_\xi]\,, \tag{2.19}$$

we do not have to solve both (2.16) and (2.17) at the same time; here we choose to solve (2.17) for $y(\xi, 0, t)$.

Then, Eqs. (2.17)–(2.18) with (2.19) serve as a complete set of exact evolution equations for y and ϕ written in the transformed plane and conserve exactly mass (m), horizontal momentum (M), and energy (E) defined by

$$m = \int y\, x_\xi \,\mathrm{d}\xi, \qquad M = \int \left(y\phi_\xi + \frac{1}{2}\Omega\, y^2 x_\xi \right) \mathrm{d}\xi, \tag{2.20}$$

$$E = \int \left[\frac{1}{3}\Omega^2 y^3 x_\xi + \Omega y^2 \phi_\xi - \phi\, \psi_\xi + g\, y^2 x_\xi + \frac{2\sigma}{\rho}\left({x_\xi}^2 + {y_\xi}^2 \right)^{1/2} \right] \mathrm{d}\xi. \tag{2.21}$$

For small amplitude waves ($x_\xi \simeq 1$ and $J \simeq 1$), by neglecting nonlinear terms, the system given by (2.17)–(2.18) can be approximated by

$$y_t = -U_0\, y_\xi - \psi_\xi, \qquad \phi_t = -U_0 \phi_\xi - gy + \Omega\psi + \frac{\sigma}{\rho}\, y_{\xi\xi}, \tag{2.22}$$

for which the linear dispersion relation between the linear wave speed c_0 and the wave number k can be found as

$$c_0 = U_0 - \frac{\Omega \tanh(kh)}{2k} \pm \left[\frac{g \tanh(kh)}{k} \left(1 + \frac{\sigma}{\rho g} k^2 \right) + \left(\frac{\Omega \tanh(kh)}{2k} \right)^2 \right]^{1/2}, \tag{2.23}$$

where we have used

$$\mathcal{T}[\mathrm{e}^{ikx}] = i \coth(kh)\, \mathrm{e}^{ikx}. \tag{2.24}$$

As a special case, for irrotational gravity waves in the absence of uniform stream ($U_0 = \Omega = \sigma = 0$), the system given by (2.17)–(2.18) can be reduced to that of Ovsjannikov (1974) [12] and Dyachenko et al. (1996) [8]:

$$y_t = y_\xi\, \mathcal{T}\left[\frac{\psi_\xi}{J} \right] - x_\xi \left(\frac{\psi_\xi}{J} \right) + U_0 \left(\mathcal{T}\left[\frac{y_\xi}{J} \right] - \frac{x_\xi}{J} \right) y_\xi, \tag{2.25}$$

$$\phi_t = -gy - \frac{1}{2J}\left({\phi_\xi}^2 - {\psi_\xi}^2 \right) + \phi_\xi\, \mathcal{T}\left[\frac{\psi_\xi}{J} \right] + U_0 \left(\mathcal{T}\left[\frac{y_\xi}{J} \right] - \frac{x_\xi}{J} \right) \phi_\xi + \frac{\sigma}{\rho} \frac{x_\xi y_{\xi\xi} - y_\xi x_{\xi\xi}}{\left({x_\xi}^2 + {y_\xi}^2 \right)^{3/2}}. \tag{2.26}$$

3. Traveling wave solutions and Benjamin–Feir instability

Here we first compute traveling wave solutions of the system given by (2.17)–(2.18) and then solve numerically the evolution of a modulated wavetrain to study the Benjamin–Feir instability. For numerical computations, we consider the infinitely deep water case ($h \to \infty$) and solve (2.17)–(2.18) with neglecting the surface tension ($\sigma = 0$).

To obtain the traveling wave solutions, we regard $-U_0$ as the speed of a wave traveling in the positive x-direction and, then, the wave becomes stationary in this reference frame. From (2.7) or (2.17), the streamfunction can be found, in terms of y, as

$$\Psi_\xi = 0, \qquad \text{or} \quad \psi_\xi = c y_\xi - \Omega y y_\xi, \tag{3.1}$$

where c is the wave speed and, from (2.19), the velocity potential is given by

$$\phi_\xi = -c\mathcal{H}[y_\xi] + \Omega\mathcal{H}[y y_\xi]. \tag{3.2}$$

By substituting (3.1)–(3.2) into (2.18), the governing equation for $y(\xi)$ can be obtained as

$$(-c + \Omega y\, x_\xi + \Omega\mathcal{H}[y y_\xi])^2 = (B - 2gy)\left({x_\xi}^2 + {y_\xi}^2 \right), \tag{3.3}$$

where, from (2.19), $x_\xi = 1 - \mathcal{H}[y_\xi]$, and the Bernoulli constant B needs to be determined. Notice that the left-hand side of Eq. (3.3) divided by $J\ (\equiv {x_\xi}^2 + {y_\xi}^2)$ represents $2q^2$ in Simmens and Saffman (1985) [15], where q is the tangential velocity at the free surface.

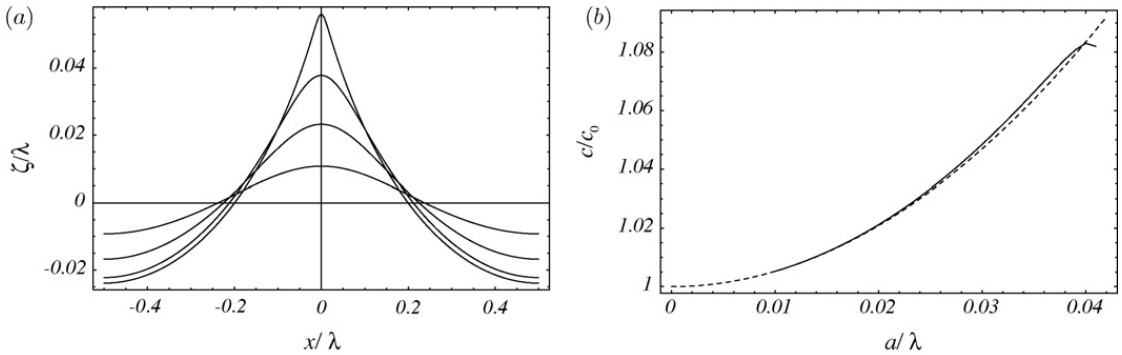

Fig. 2. Numerical solutions of (3.3)–(3.4) for periodic traveling waves with $\Omega/\omega = 1/2$, where ω is the irrotational wave frequency given by $\omega = (2\pi g/\lambda)^{1/2}$: (a) wave profiles for $a/\lambda = 0.01,\ 0,02,\ 0.03,\ 0.04$; (b) wave speed versus wave amplitude compared with the weakly nonlinear result (- - -) given by (3.7).

By using the Newton–Raphson method, as described in Choi and Camassa (1999) [5] for the case of $\Omega = 0$, we iteratively solve (3.3) with an error tolerance smaller than 10^{-7} and the number of Fourier modes is $N = 2^7 – 2^8$. For given wave height $2a$ and wavelength λ, when (3.3) is discretized at N discrete points using a pseudo-spectral method, there are $N + 2$ unknowns (y_j, c, B) for $j = 1, 2, \cdots, N$. Two additional equations used in our computations are

$$y(0) - y(\lambda/2) = 2a, \qquad \int_0^{\lambda/2} y x_\xi \, \mathrm{d}\xi = 0, \tag{3.4}$$

where the first equation is the definition of wave height, and the second equation implies that the mean surface level in the physical plane vanishes. As an initial guess for this iterative procedure, we use the weakly nonlinear solutions correct to the second order in wave steepness given, from Simmen and Saffman (1985) [15], by

$$y = a_1 \cos(kx) + a_2 \cos(2kx) + \cdots, \qquad c = c_0 + c_2 + \cdots, \qquad a = a_1 + a_2 + \cdots, \tag{3.5}$$

where

$$a_2 = \frac{1}{2{c_0}^2 k}\left({c_0}^2 k^2 + 2\Omega c_0 k + \frac{1}{2}\Omega^2\right){a_1}^2, \tag{3.6}$$

$$c_2 = \frac{1}{2{c_0}^2 k(2c_0 k + \Omega)}\left[{c_0}^4 k^4 - \frac{1}{2}\Omega^2 {c_0}^2 k^2 + \left({c_0}^2 k^2 + 2\Omega c_0 k + \frac{1}{2}\Omega^2\right)^2\right]{a_1}^2. \tag{3.7}$$

Figs. 2 and 3 show the computed wave profiles and wave speeds for $\Omega/\omega = \pm 1/2$, respectively, where $\omega = (2\pi g/\lambda)^{1/2}$ is the irrotational wave frequency. For $\Omega/\omega = 1/2$, the computed maximum wave amplitude and the maximum wave speed are $a_{\max}/\lambda \simeq 0.0410$ and $c_{\max}/(g\lambda)^{1/2} \simeq 0.3370$, which are in good agreement with those of Simmen and Saffman (1985) [15], $a_{\max}/\lambda \simeq 0.0412$ and $c_{\max}/(g\lambda)^{1/2} \simeq 0.3372$. For $\Omega/\omega = -1/2$, the computed maximum wave

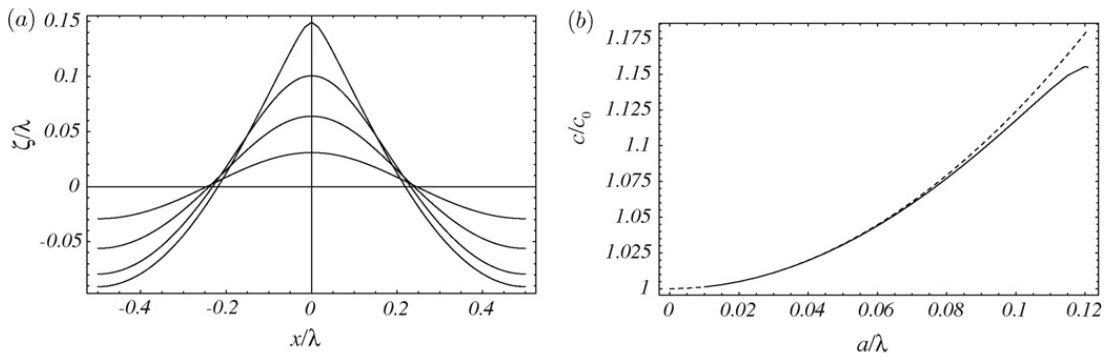

Fig. 3. Numerical solutions of (3.3)–(3.4) for periodic traveling waves with $\Omega/\omega = -1/2$: (a) wave profiles for $a/\lambda = 0.03,\ 0,06,\ 0.09,\ 0.12$; (b) wave speed versus wave amplitude compared with the weakly nonlinear result (- - -) given by (3.7).

amplitude and the maximum wave speed are $a_{\max}/\lambda \simeq 0.1208$ and $c_{\max}/(g\lambda)^{1/2} \simeq 0.5899$, respectively, which are comparable to those of Simmen and Saffman (1985) [15], $a_{\max}/\lambda \simeq 0.1226$ and $c_{\max}/(g\lambda)^{1/2} \simeq 0.5896$.

Compared with the maximum wave amplitude, $a_{\max}/\lambda \simeq 0.0702$, in the absence of shear, the maximum wave amplitude is much smaller for positive Ω and larger for negative Ω. This observation is consistent with the recent laboratory experiment of Yao and Wu (2005) [20] where the wave steepness at incipient breaking is observed to be smaller for the case of positive shear ($\Omega > 0$) than the case of $\Omega = 0$. The opposite is observed to be true for negative Ω. It is interesting to notice that the wave speed from the weakly nonlinear theory matches well with the fully nonlinear numerical solution far beyond the weakly nonlinear regime although the second-order solutions are a poor approximation to the exact wave profiles.

To excite the Benjamin–Feir instability, as an initial condition for the free surface elevation, we consider a wave train whose amplitude is slightly modulated so that the free surface elevation y in the physical space is given by

$$y(x, 0) = [1 + A\cos(Kx)]\, y_s(x), \tag{3.8}$$

where y_s represents the computed traveling wave solution of wave height $2a$ and wavelength λ, and $L = 2\pi/K$ is the wavelength of the envelope. This initial condition is equivalent to adding small perturbations at two sidebands of wave numbers of $k - K$ and $k + K$. Initially, we assume that there is no perturbation to the free surface velocity potential for

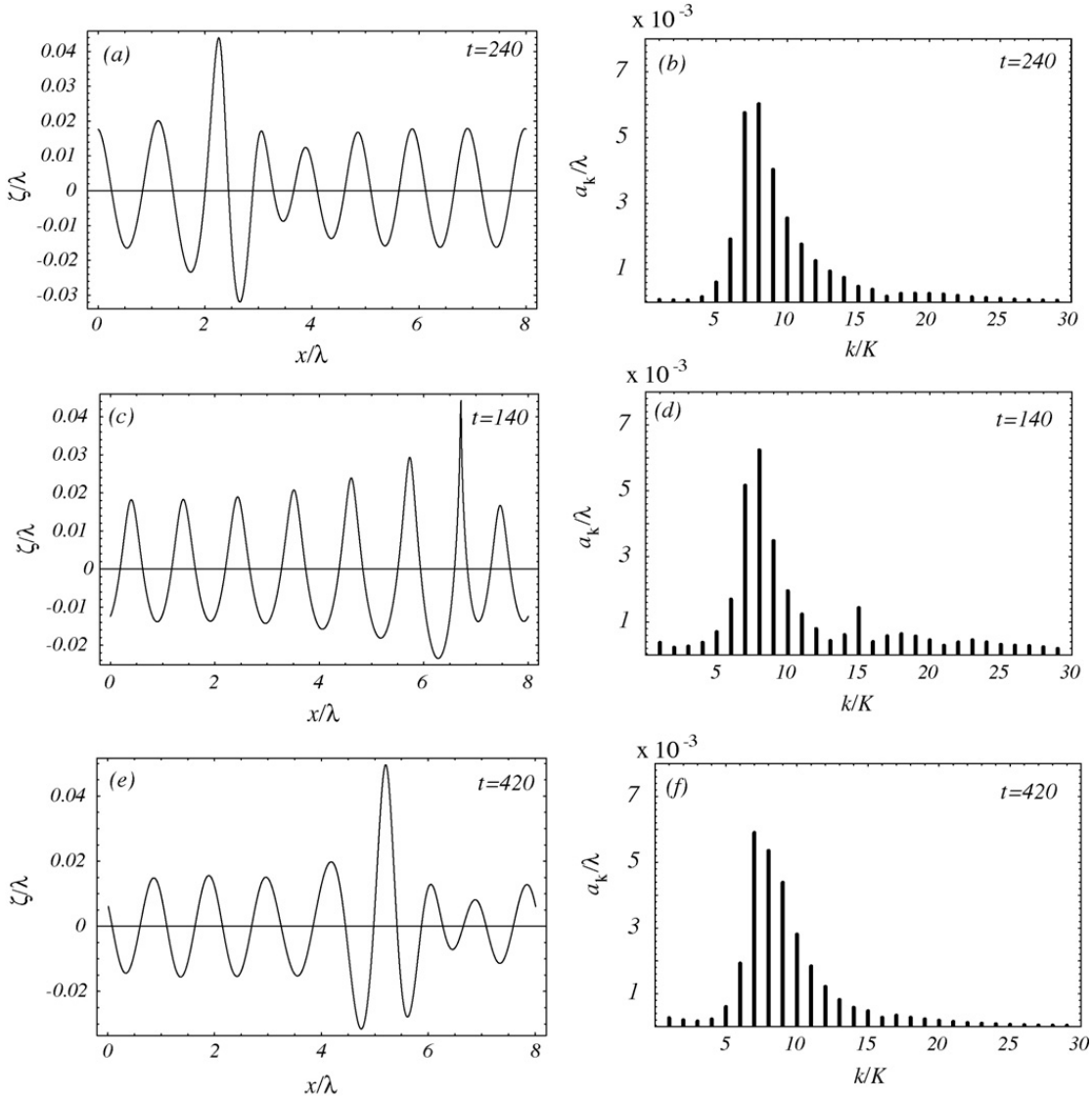

Fig. 4. Benjamin–Feir instability: Numerical solutions of (2.17)–(2.18) in a frame of reference moving with the wave speed for the initial condition given by (3.8). (a) and (b): The free surface elevation and its Fourier coefficients for $\Omega/\omega = 0$; (c) and (d): $\Omega/\omega = 1/2$; (e) and (f): $\Omega/\omega = -1/2$.

the traveling wave solution. In our computations, we choose $\lambda = 1$, $g = 1$, $a = 0.02$, $A = 0.1$, and $L = 8$. The total number of Fourier modes is $N = 2^{10} = 1024$ ($2^7 = 128$ nodes per wavelength) and the time step is $\Delta t = 0.001$. For numerical solutions shown in this paper, mass, horizontal momentum and energy are conserved to $O(10^{-3}\%)$.

Fig. 4 shows the free surface elevation and its Fourier coefficients for $\Omega/\omega = 0$, 1/2, $-1/2$ at the time when the Fourier coefficient of the lower side-band ($k/K = 7$) grows to become approximately comparable to that of the primary wavenumber ($k/K = 8$) for the first time (known as the frequency downshift). Notice that, for a fixed initial wave slope ($a/\lambda = 0.02$), the growth rate of an unstable wave envelope is greater for positive Ω than that for the case of $\Omega = 0$ while the opposite is true for negative Ω. Thus, it can be concluded that a positive shear current enhances the Benjamin–Feir instability. As shown in Fig. 4(c) and (d), the higher harmonics have relatively higher amplitudes for positive Ω and the peak of the envelope gets much steeper.

4. Conclusion

We have derived a system of exact evolution equations for surface waves propagating in a linear shear current. Both steady and unsteady gravity waves are studied numerically for infinitely deep water by solving the system using a pseudo-spectral method.

It is found that both steady and unsteady waves reveal stronger nonlinear wave characteristics at smaller wave amplitudes for the case of a positive shear (or, equivalently, negative vorticity) than for the negative or zero shear case. Although the infinite depth case is considered for our numerical computations, the current at a great depth affects little the wave motion that decays exponentially with depth and, therefore, the same conclusion is expected to be made for the finite depth case as long as the wavelength is smaller than water depth.

The approach presented in this paper can be applied only to a current with constant vorticity. A more general vorticity distribution could be approximated by a multi-layer model proposed by [16], where the vorticity is constant in each layer. Such a multi-layer model has been successfully used in other flow problems, e.g., density-stratified flows and, therefore, an extension of the present formulation might be useful although careful validation with laboratory experiments is required.

Acknowledgements

The author gratefully acknowledges support from the US Office of Naval Research through Grant N00014-05-1-0537. The author is grateful to Chin H. Wu for useful discussions.

References

[1] M.L. Banner, J.-B. Song, On determining the onset and strength of breaking for deep water waves. Part II: influence of Wind Forcing and Surface Shear, J. Phys. Oceanogr. 32 (2002) 2559–2570.
[2] M.L. Banner, X. Tian, On the determination of the onset of breaking for modulating surface gravity water waves, J. Fluid Mech. 367 (1998) 107–137.
[3] T.B. Benjamin, The solitary wave on a stream with an arbitrary distribution of vorticity, J. Fluid Mech. 12 (1962) 97–116.
[4] W. Choi, Strongly nonlinear long gravity waves in uniform shear flows, Phys. Rev. E 68 (2003) 026305.
[5] W. Choi, R. Camassa, Exact evolution equations for surface waves, J. Eng. Mech. 125 (1999) 756–760.
[6] R.A. Dalrymple, A finite amplitude wave on a linear shear current, J. Geophys. Res. 79 (1974) 4498–4504.
[7] J.W. Dold, D.H. Peregrine, Water-wave modulation, in: Proc. 20th. Intl. Conf. Coastal Engng., vol. 1, 1986, pp. 163–175.
[8] A.L. Dyachenko, V.E. Zakharov, E.A. Kuznetsov, Nonlinear dynamics of the free surface of an ideal fluid, Plasma Phys. Rep. 22 (1996) 916–928.
[9] Y.A. Li, J.M. Hyman, W. Choi, A numerical study of the exact evolution equations for surface waves in water of finite depth, Stud. Appl. Math. 113 (2004) 303–324.
[10] V.A. Miroshnikov, The Boussinesq-Rayleigh approximation for rotational solitary waves on shallow water with uniform vorticity, J. Fluid Mech. 456 (2002) 1–32.
[11] M. Okamura, M. Oikawa, The linear stability of finite amplitude surface waves on a linear shearing currents, J. Phys. Soc. Jpn. 58 (1989) 2386–2396.
[12] L.V. Ovsjannikov, To the shallow water theory foundation, Arch. Mech. 26 (1974) 407–422.
[13] D.H. Peregrine, Interaction of water waves and currents, Adv. App. Mech. 16 (1976) 9–117.
[14] D. Pullin, R.H.J. Grimshaw, Stability of finite-amplitude interfacial waves. III The effect of basic current shear, J. Fluid Mech. 172 (1986) 277–306.

[15] J.A. Simmen, P.G. Saffman, Steady deep-water waves on a linear shear current, Stud. Appl. Math. 73 (1985) 35–57.
[16] C. Swan, I.P. Cummins, R.L. James, An experimental study of two-dimensional surface water waves propagating on depth-varying currents. Part 1, Regular waves. J. Fluid Mech. 428 (2001) 273–304.
[17] A.F. Teles da Silva, D.H. Peregrine, Steep, steady surface waves on water of finite depth with constant vorticity, J. Fluid Mech. 195 (1988) 281–302.
[18] J.-M. Vanden-Broeck, Steep solitary waves in water of finite depth with constant vorticity, J. Fluid Mech. 274 (1994) 339–348.
[19] J.-M. Vanden-Broeck, Periodic waves with constant vorticity in water of infinite depth, IMA J. Appl. Math. 56 (1996) 207–217.
[20] A. Yao, C.H. Wu, Incipient breaking of unsteady waves on sheared currents, Phys. Fluids 17 (2005) 082104.